Journal of Power Sources 202 (2012) 374–379

Contents lists available at SciVerse ScienceDirect

Journal of Power Sources

journal homepage: www.elsevier.com/locate/jpowsour

Short communication

Low-temperature synthesis of nano-micron $Li_4Ti_5O_{12}$ by an aqueous mixing technique and its excellent electrochemical performance

Feixiang Wu, Xinhai Li*, Zhixing Wang, Huajun Guo, Zhenjiang He, Qian Zhang, Xunhui Xiong, Peng Yue

School of Metallurgical Science and Engineering, Central South University, Changsha 410083, PR China

ARTICLE INFO

Article history:
Received 26 September 2011
Received in revised form
12 November 2011
Accepted 15 November 2011
Available online 25 November 2011

Keywords:
Lithium ion batteries
Lithium titanate
Nano-micron materials
Anode material
Spray drying

ABSTRACT

We demonstrate an aqueous mixing technique to synthesize nano-micron $Li_4Ti_5O_{12}$ by spray drying followed by solid-state calcination. The as-prepared materials are characterized by XRD, TG–DTA, SEM, TEM and electrochemical measurements. Well-crystallized $Li_4Ti_5O_{12}$ with no impurity can be obtained at a relatively low calcined temperature (650 °C) owing to the effect of nanoscale and uniform particles. Because of the rough and porous nano-micron spherical particles, the obtained $Li_4Ti_5O_{12}$ shows excellent rate capability and cycle ability. The initial discharge capacities are 174.8, 170.5, 167.5, 165.3, 158.2, 152.1, 130.9 and 111.9 mAh g^{-1} at the 0.1, 0.5, 1, 2, 5, 10, 15 and 20 *C* rates, respectively. After 100 cycles, the as-prepared $Li_4Ti_5O_{12}$ retains 99.6%, 96.9%, 98.8%, 89.3%, 90.4% and 89.0% of its initial discharge capacities at the 1, 2, 5, 10, 15 and 20 *C* rates, respectively.

1. Introduction

Rechargeable lithium-ion cells are key components of the portable, entertainment, computing, and telecommunication equipment because of their high-energy storage density, high voltage, long cycle life, high-power sources, and ambient temperature operation [1,2]. In this area, cathode materials have been widely studied, such as $LiMn_2O_4$, $LiCoO_2$, $LiNi_{1/3}Mn_{1/3}Co_{1/3}O_2$, $LiFePO_4$, etc. [3–8]. The anode materials also play an important role in the lithium-ion batteries. However, the performance of current lithium ion batteries cannot meet the requirements in these areas in terms of high power density, long cycle life, and safety. Graphite is widely used as the anode material for Li-ion batteries. The carbon negative electrode used in rechargeable lithium-ion cells suffers from a number of problems; most notably the potential for lithium intercalation is close to that of the Li^+/Li redox couple, leading to the possibility of lithium plating during charge and hence significant safety concerns, also charge must be consumed in order to form the SEI layer (essential to the operation of the carbon electrode) on the first charge cycle. The stability of the SEI can greatly impact the battery's capacity and power retention as well as cycle life [9–13]. Also the graphite anode undergoes a 9 vol% variation during full lithium insertion and extraction.

Spinel $Li_4Ti_5O_{12}$ is a promising anode material for lithium-ion batteries. The excellent cycling performance and long life of the spinel $Li_4Ti_5O_{12}$ make it a candidate as an anode electrode especially for larger scale applications such as all solid-state lithium-ion batteries and hybrid supercapacitors [14–16]. The material has a high Li-ion intercalation and deintercalation reversibility and almost exhibits no volume change during charge and discharge, which makes it a "zero strain" insertion material [14]. Spinel $Li_4Ti_5O_{12}$ has a flat Li^+ insertion potential at about 1.55 V (versus Li^+/Li) [17–19], which is above the reduction potential of electrolyte solvents, thus it can restrain the SEI film from the reduction of electrolytes and sufficiently avoid the formation of metallic lithium [14]. This material accommodates Li^+ with a theoretical capacity of 175 mAh g^{-1}. Owing to the relatively high lithium insertion potential and low theoretical capacity, the energy density of the battery using $Li_4T_5O_{12}$ will decrease significantly. However, the improved safety and reliability of the spinel compared with that of carbon electrodes make the lithium-ion batteries using $Li_4Ti_5O_{12}$ material as anode suitable to electric vehicle (EV) and power storage batteries.

$Li_4Ti_5O_{12}$ is conventionally prepared by solid-state synthesis using TiO_2 and Li_2CO_3 or LiOH and firing at 800–1000 °C for 12–24 h [20–26]. However, such solid-state synthesis results in large particle size in submicron to micron range and impurities in the obtained materials. Therefore, several researchers focused on synthesis of nanocrystalline and high purity $Li_4Ti_5O_{12}$ powder by low temperature processes like sol–gel [27–30], spray drying [31–35], hydrothermal [36,37]. These methods mix Ti and Li evenly and then

* Corresponding author. Tel.: +86 731 88836633; fax: +86 731 88836633.
E-mail address: feixiang0929@163.com (X. Li).

0378-7753/$ – see front matter © 2011 Elsevier B.V. All rights reserved.
doi:10.1016/j.jpowsour.2011.11.050

calcine to synthesize high purity and nanocrystalline $Li_4Ti_5O_{12}$. It is well known that use of nanocrystalline materials (20–100 nm) as electrode reduces the diffusion route leading to improved rate capability. In this paper, the method using H_2O_2 as coordination agent is grafted on to the preparation of nano-micron $Li_4Ti_5O_{12}$ by spray drying of lithium titanium peroxide solution. Actually, the availability of H_2O_2 to Ti compound has been well-known. The method using H_2O_2 as coordination agent is widely used in catalyst and photocatalysis fields to obtain nanosize TiO_2 thin film [38–40]. In our previous study, we use hydrogen peroxide as a coordination agent which provides a kind of ligand (O_2^{2-} ion) to dissolve Ti from the hydrolyzed titania precipitate. Several O_2^{2-} ions react with the Ti of high-titanium precipitate to form a large anion in which Ti is taken as the central ion and exist stably in the alkaline solution. The H_2O_2 as coordination agent has been grafted on to the leaching of hydrolyzed titania residue decomposed from mechanically activated Panzhihua ilmenite leached by hydrochloric acid and preparation of TiO_2 nanowires as an anode material for lithium-ion batteries [41,42]. Owing to this special lithium titanium peroxide solution, we can get the nano-micron precursor of $Li_4Ti_5O_{12}$, in which the Ti and Li are evenly mixed. After that, we can obtain as-prepared $Li_4Ti_5O_{12}$ at lower temperature than before. Furthermore, the obtained nano-micron $Li_4Ti_5O_{12}$ shows excellent electrochemical performance.

2. Experimental

2.1. Synthesis and characterization

In this experiment, nano-micron $Li_4Ti_5O_{12}$ was fabricated by spray drying of lithium titanium peroxide solution, followed by solid-state calcination. The special lithium titanium peroxide was obtained at room temperature. Firstly, 30 g of $Ti(OC_4H_9)_4$ was added into 100 ml de-ionized water and white slurry was observed. After stirring for 5 min, 60 g of 30 wt.% H_2O_2 solution was added into the slurry followed by ammonia solution (12.5 wt.%) that maintains pH value near 10. After 20 min, the white slurry was dissolved to form a yellow-green solution A. Secondly, 3.0801 g of 96 wt.% $LiOH{\cdot}H_2O$ was added into 50 ml de-ionized water, and then obtained the lithium hydroxide solution B. At last, solutions A and B were added into 500 ml de-ionized water in the 1000 ml beaker and then stirred for 10 min. The prepared precursor solution was spray drying by spray drier machine (SD-2500). The solution was added into the spray drier machine by peristaltic pump at the 300 ml h^{-1}. The homogenous solution was atomized at 200 °C using a two-fluid nozzle with atomizing pressure of 0.2 MPa. The spray-dried precursor powders were further calcined in air at 650 °C for 16 h to form $Li_4Ti_5O_{12}$ particles. The experimental procedure and spray drying apparatus were shown in Fig. 1.

The precursor was analyzed by using a simultaneous TG–DTA apparatus SDT Q600 (TA instruments). The SEM images of the particles were observed with scanning electron microscopy (SEM, Sirion 200). The powder X-ray diffraction (XRD, Rint-2000, Rigaku) using Cu Kα radiation was employed to identify the crystalline phase of the precursor and nano-micron $Li_4Ti_5O_{12}$.

2.2. Electrochemical measurement

The electrochemical performance was performed using a two-electrode coin-type cell (CR2025) of Li|$LiPF_6$ (EC:EMC:DMC = 1:1:1 in volume)|$Li_4Ti_5O_{12}$. The working cathode was composed of 80 wt.% $Li_4Ti_5O_{12}$ powders, 10 wt.% acetylene black as conducting agent, and 10 wt.% poly (vinylidene fluoride) as binder. After being blended in N-methyl pyrrolidinone, the mixed slurry was spread uniformly on a thin copper foil and dried in vacuum for 12 h at 120 °C. A metal lithium foil was used as the anode. Electrodes were punched in the form of 14 mm diameter disks, and the typical positive electrode loading was about 1.95 mg cm^{-2}. A polypropylene micro-porous film was used as the separator. The assembly of the cells was carried out in a dry argon-filled glove box. The cells were charged and discharged over a voltage range of 1.0–2.5 V versus Li/Li^+ electrode at room temperature.

3. Results and discussion

3.1. Morphology and structure of the materials

Fig. 2(a) shows TG/DTA curves of the precursor which is obtained by spray drying the special lithium titanium peroxide solution. From curves of TG/DTA, it can be clearly seen that there are two distinct steps of weight loss. The first step of weight loss of 12.12% corresponding to the first endothermic peak at 106.7 °C occurs from room temperature to 200 °C on the TG–DTA curves due to the vaporization of adsorbed water molecules in the precursor. The FT-IR curves for as-dried powders of precursor and the precursor calcined at 350 °C for 3 h are shown in Fig. 2(b). Both spectra are similar each other. The broad peak appearing at 3100–3600 cm^{-1} is assigned to the fundamental stretching vibration of hydroxyl groups (free or bonded), which is further confirmed by the weak band at about 1620 cm^{-1}. This absorption band is caused by the bending vibration of coordinated H_2O as well as Ti–OH and Li–OH. The peak at 1400 cm^{-1} was attributed to the stretching vibration of the N···H bonds in NH_4^+ remained [43]. Corresponding to results of FT-IR curves, the second weight loss of 18.08% and endothermic peak, which is mainly attributed to decomposition of the N–H, Ti–OH and Li–OH bonds, is from 200 to 550 °C in the TG–DTA curves. Fig. 2(c) shows the X-ray diffraction (XRD) patterns of the precursor and as-prepared $Li_4Ti_5O_{12}$. The precursor has no peaks, indicating no appearance of crystalline phases. The as-prepared $Li_4Ti_5O_{12}$ is single-phase spinel lithium titanium oxide (cubic phase, space group *Fd-3m*) in accordance with spinel $Li_4Ti_5O_{12}$ (JCPDS Card No. 49-0207) and well crystallized. It means that we can get well crystallized and single phase of $Li_4Ti_5O_{12}$ at relatively low temperature of 650 °C by calcining precursor prepared by this method.

Fig. 3 shows the SEM (a, b) and TEM (c, d) images of the precursor at different magnifications. The precursor powders are characterized by the spherical morphology with the particle size of about 1–5 μm. From Fig. 3(a–c), the surface of the precursor is smooth, which has been magnified in Fig. 3(d). The spherical particles contain lots of nanoparticles with size of several nanometers. Owing to the effect of these nanoscale and uniform particles, we can obtain the high purity $Li_4Ti_5O_{12}$ at relatively low calcined temperature. There is no obvious circle in the SAED pattern indicating no appearance of crystalline phases, which is well in accordance with the XRD result of precursor. After calcined at 650 °C for 16 h, the as-prepared $Li_4Ti_5O_{12}$ also shows uniform and spherical structure morphology with the same size as the precursor. However, owing to the decomposition of precursor, the surface of spherical particles changes into rough and porous surface which is constituted with aggregations of nanoparticles with the size of about 100 nm (Fig. 4(a and b)). The SAED pattern in Fig. 4(c), with several marked rings corresponding to $Li_4Ti_5O_{12}$ (1 1 1), (3 1 1), (4 0 0) and (4 4 0) planes, can be indexed to spinel $Li_4Ti_5O_{12}$ with the cubic space group *Fd-3m*. Fig. 4(d) shows the HRTEM images of as-prepared $Li_4Ti_5O_{12}$ nanoparticles. As can be seen, there is a lattice fringe with a lattice spacing of about 0.48 nm, corresponding to (1 1 1) interplanar spacing of $Li_4Ti_5O_{12}$, which indicates the well-crystallized spinel phase in the nanostructured materials prepared from relatively low temperature heat treatment.

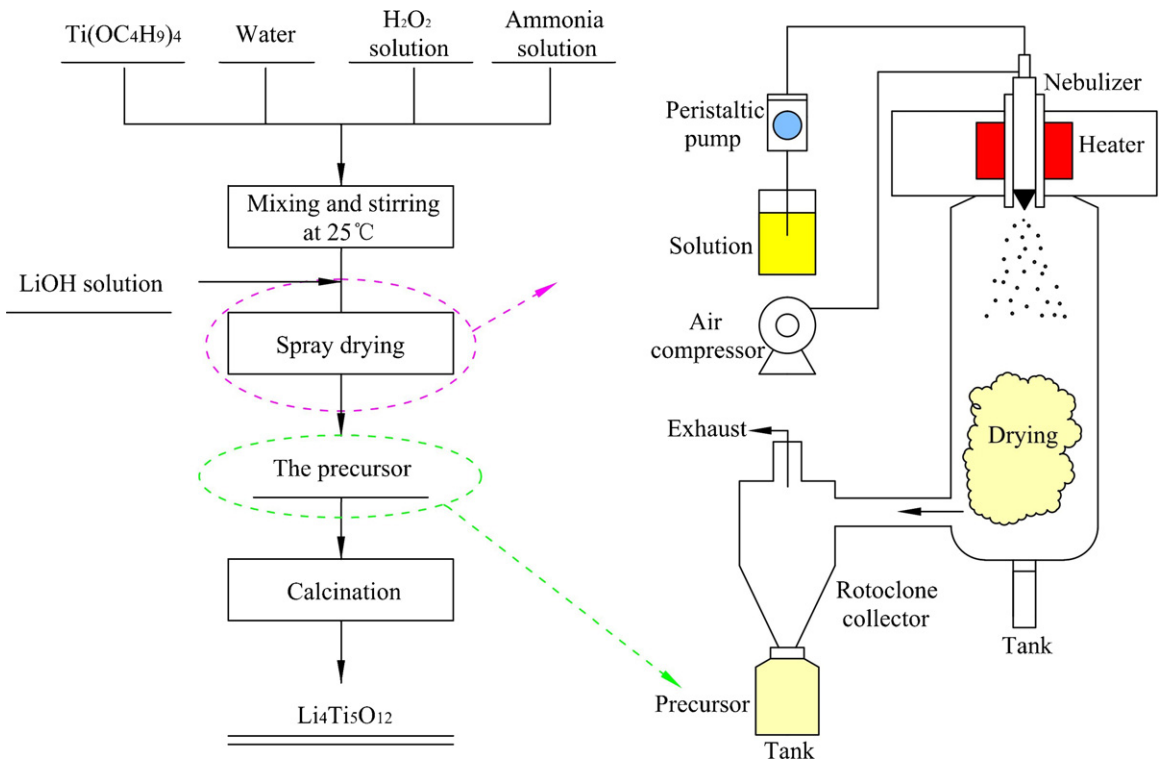

Fig. 1. The experimental procedure and spray drying apparatus.

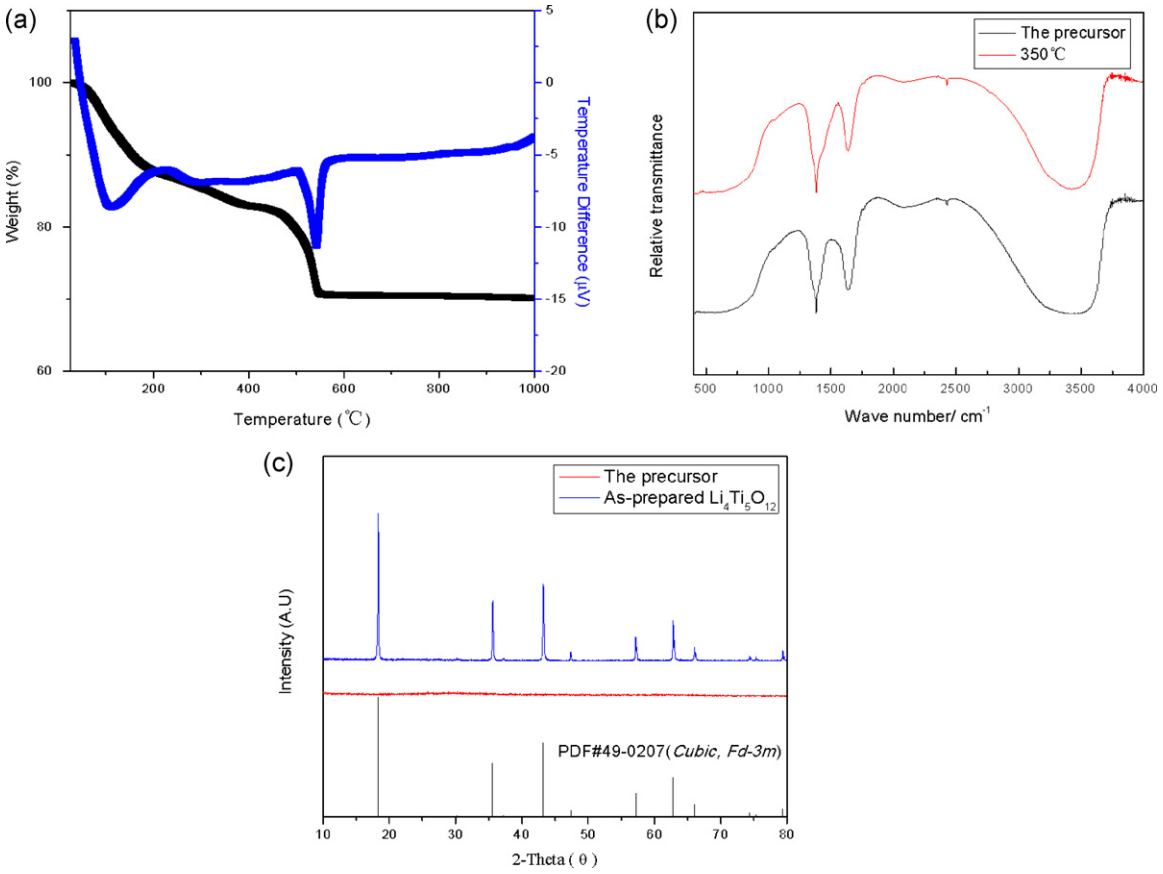

Fig. 2. (a) The TG/DTA curves of the precursor; (b) FT-IR curves for the precursor and the precursor calcined at 350 °C for 3 h and (c) XRD patterns of the precursor and as-prepared $Li_4Ti_5O_{12}$.

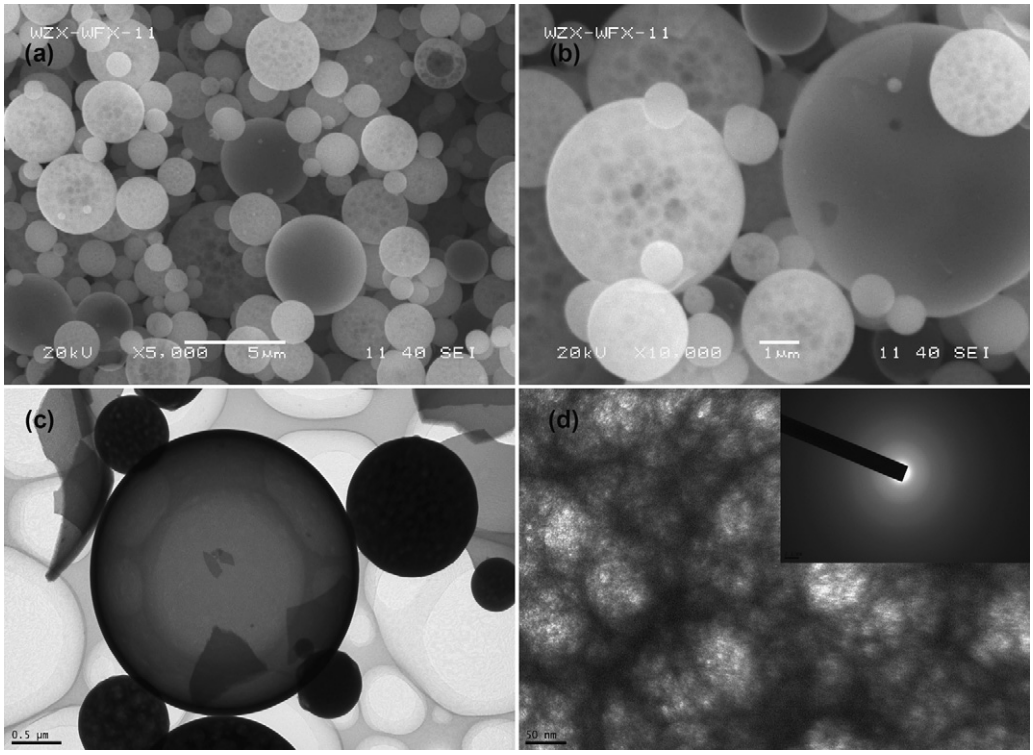

Fig. 3. SEM (a and b) and TEM (c and d) images of the precursor at different magnifications (inset: SAED pattern taken from the precursor).

3.2. Electrochemical performance

Rates of up to 20 *C* rate have been investigated to evaluate as-prepared $Li_4Ti_5O_{12}$ electrode and the results are shown in Fig. 5(a). The cell was first cycled at *C*/10 for 3 cycles, *C*/2 for 6 cycles, 1 *C* for 100 cycles, 2 *C* for 100 cycles, 5 *C* for 100 cycles, 10 *C* for 100 cycles, 15 *C* for 100 cycles and then turned to 20 *C* for 100 cycles. At all the *C*-rates, the charge/discharge curves exhibit a long and flat voltage plateaus. In the first discharge process, the as-prepared $Li_4Ti_5O_{12}$ electrode exhibits a remarkably high

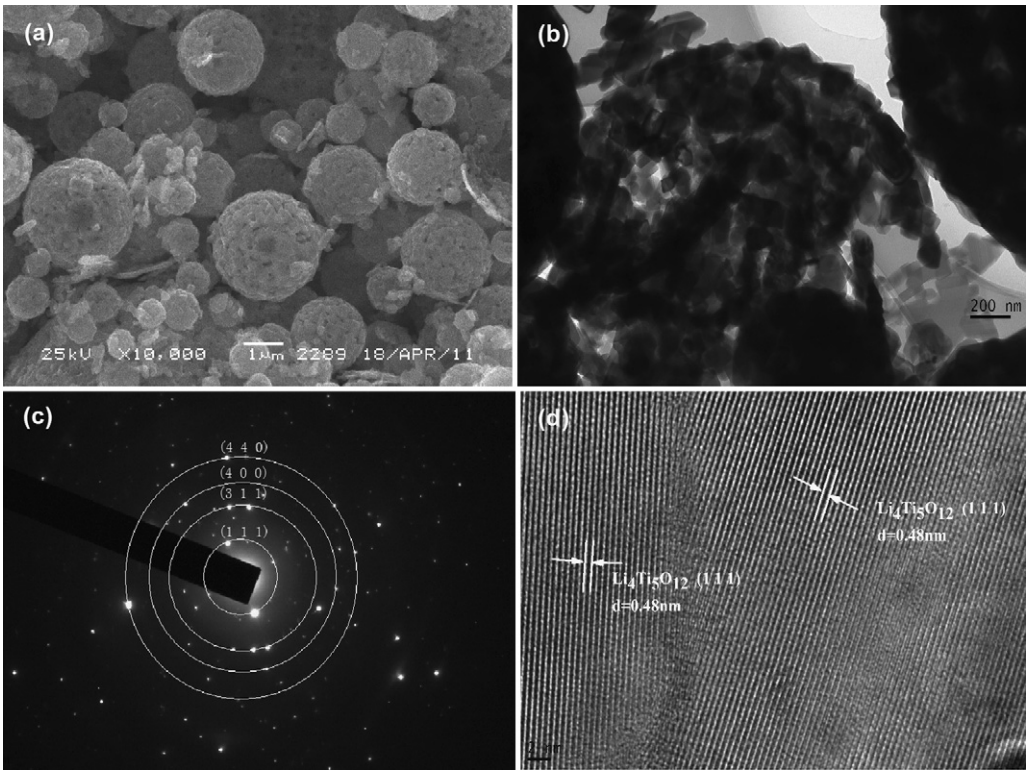

Fig. 4. SEM (a), TEM (b), SAED (c) and HRTEM (d) images of as-prepared $Li_4Ti_5O_{12}$.

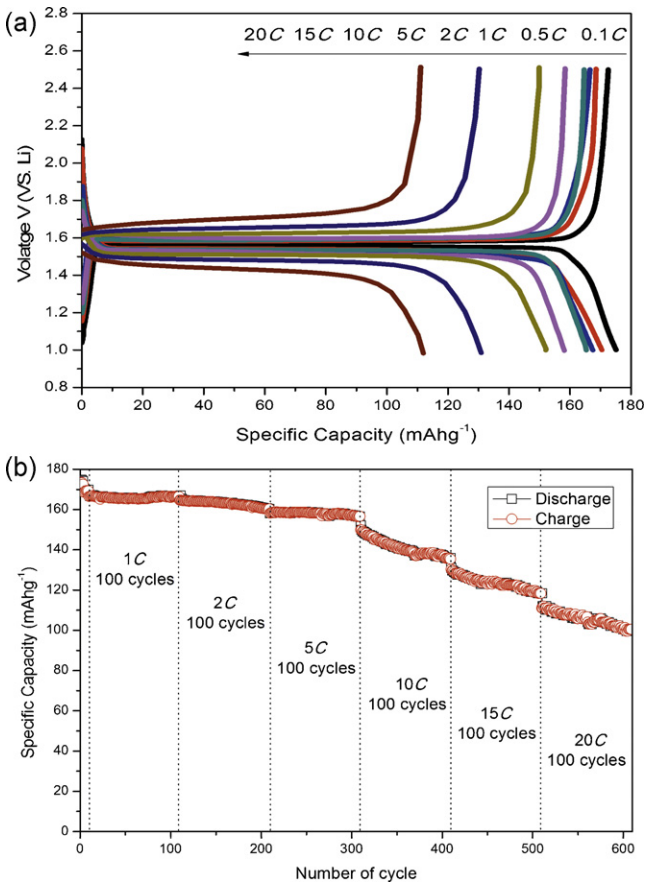

Fig. 5. (a) The initial charge/discharge curves of $Li_4Ti_5O_{12}$ at different *C*-rates in the voltage range of 1.0–2.5 V and (b) cycling performance of $Li_4Ti_5O_{12}$ at different *C*-rates.

initial discharge capacity at 0.1 *C* rate, up to 174.8 mAh g^{-1}, which is almost equal to its theoretical capacity (175 mAh g^{-1}). The subsequent Li^+ extraction, proceeding up to 2.5 V, shows a capacity of 172.8 mAh g^{-1}, with a high columbic efficiency (ratio of extraction to insertion capacity) of 98.85%. By increasing the *C*-rate, the cell shows 170.5, 167.5, 165.4, 158.2, 152.1, 130.9 and 111.9 mAh g^{-1} at 0.5, 1, 2, 5, 10, 15 and 20 *C* rates, respectively. The capacities at all charge/discharge rates are much larger than other $Li_4Ti_5O_{12}$ and $Li_4Ti_5O_{12}$/C electrodes [20–37]. Moreover, the cycling performance of as-prepared $Li_4Ti_5O_{12}$ is shown in Fig. 5(b). As shown, the cycling curves of discharge and charge are coincided with each other, indicating a high coulombic efficiency in the charge/discharge of this cell. At all the current densities, after 100 cycles, the as-prepared $Li_4Ti_5O_{12}$ electrode retains 99.6%, 96.9%, 98.8%, 89.3%, 90.4% and 89.0% of its initial discharge capacities at the 1, 2, 5, 10, 15 and 20 *C* rates, respectively. The excellent electrochemical performance might be attributed to as-prepared special nano-micron $Li_4Ti_5O_{12}$ obtained by this novel method. The nano-micron $Li_4Ti_5O_{12}$ can not only supply shorter transport length for Li^+ and electronic transport within the particles, but also make a larger electrode–electrolyte contact area for Li^+ insertion/extraction. Owing to the high purity, well-crystallized, nanosizing, rough and porous spherical particles, the as-prepared $Li_4Ti_5O_{12}$ shows excellent high-rate and cycling performance.

Cyclic voltammograms of $Li_4Ti_5O_{12}$ at the scan rates of 0.1, 0.2, 0.5, 1 and 2 mV s^{-1} between 2.5 and 1 V are shown in Fig. 6. Only one oxidation/reduction peak is observed, which is coincided with the single phase of $Li_4Ti_5O_{12}$ after the calcination at 650 °C as shown in Fig. 2(b). The cathodic peak locates around 1.5 V at 0.1 mV s^{-1}, which moves steady to the lower voltage with the increase of

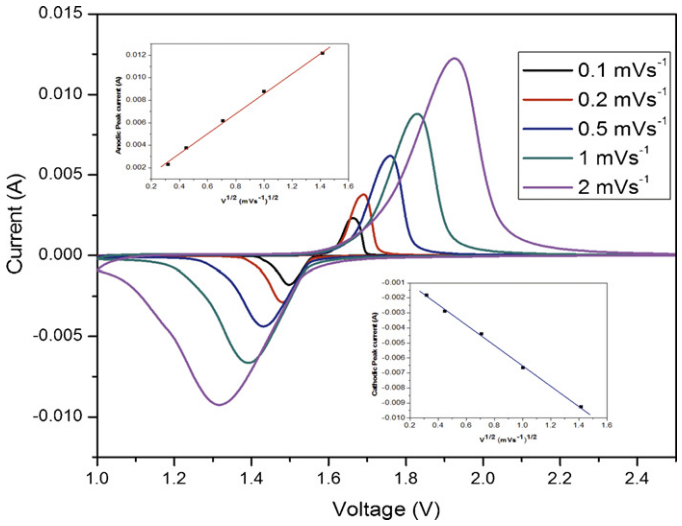

Fig. 6. Cyclic voltammograms of the as-prepared $Li_4Ti_5O_{12}$ at different scan rates. The relationships between the peak current and square root of scan rate in the cathodic and anodic processes are instead into figure.

scanning rate, corresponds to the voltage platform of the discharge process in which Li^+ intercalate into the spinel $Li_4Ti_5O_{12}$. The anodic peak at 1.66 V corresponds to the voltage platform of the charge process in which Li^+ de-intercalate from the spinel $Li_7Ti_5O_{12}$. It is well known that the relation between peak currents and scan rates indicates the different electrochemical reaction characteristics, including solid phase diffusion-controlled or surface-confined charge-transfer processes [44–46]. As shown in Fig. 6, there is a linear relationship between cathodic/anodic current peak and square root of scan rate, which shows the diffusion controlled reaction for cathodic and anodic processes. It is well known that the linear equation is $I_{pa/pc} = 2.69 \times 10^5 An^{2/3}C_0D^{1/2}v^{1/2}$ (at 25 °C) [47] where $I_{pa/pc}$, the peak currents of cathodic and anodic peaks; *n*, the number of electrons per molecule during the intercalation; *A*, the surface area of the anode (geometric surface area of the electrode is used instead); C_0, the concentration of lithium ions; *D*, the diffusion coefficient of lithium ion and *v* is the scan rate. According to the linear equation, the calculated $D_{reduction}$, $D_{oxidation}$ and $D_{average}$ are 1.65×10^{-8}, 8.32×10^{-9} and 1.241×10^{-8} cm^2 s^{-1}, respectively, which are at the range of 2×10^{-8} to 2×10^{-12} cm^2 s^{-1} and consistent with the results reported by Rho and Kanamura [48]. The as-prepared $Li_4Ti_5O_{12}$ in the voltage platform of discharge state shows higher lithium-ion diffusion coefficient than it of the sample in the voltage platform of charge state, which in accordance with the result reported by Yuan and Cai [49]. The variation of Li^+ diffusion coefficient reported by different researchers suggests that the synthesis technique has significant effect on the Li^+ transportation inside the electrode.

4. Conclusions

In summary, the nano-micron $Li_4Ti_5O_{12}$ is successfully synthesized by a simple method using an aqueous mixing technique. Owing to the special lithium titanium peroxide solution, the precursor obtained by spray drying can be calcined at relatively low temperature (650 °C) to obtain well-crystallized, rough and porous nano-micron spherical particles $Li_4Ti_5O_{12}$ which shows excellent electrochemical performance. As above mentioned, this novel aqueous mixing method is a promising technique to prepare $Li_4Ti_5O_{12}$. Actually, we can use inorganic compounds of titanium to prepare the lithium titanium peroxide solution, which can reduce the cost of preparation. In addition, we can add carbon (or

metals) compounds into the special lithium titanium peroxide solution to synthesize $Li_4Ti_5O_{12}$/C or metals doped $Li_4Ti_5O_{12}$ by this novel method, which we will report in the future. This high-rate performance nano-micron anode material coupled with the simple, relatively low temperature, low cost, and environmentally benign nature of the preparation method may make this material attractive for large applications in high-performance rechargeable lithium ion batteries and high-power electrochemical supercapacitors.

Acknowledgements

The project was sponsored by the Major Special Plan of Science and Technology of Hunan Province, China (Grant No. 2011FJ1005).

References

[1] J.M. Tarascon, M. Armand, Nature 414 (2001) 359.
[2] M.S. Whittingham, Chem. Rev. 104 (2004) 4271.
[3] Y.K. Li, R.X. Zhang, J.S. Liu, J. Power Sources 189 (2009) 685.
[4] Z.H. Chen, J.R. Dahn, Electrochim. Acta 49 (2004) 1079.
[5] F. Zhou, W.B. Luo, X.M. Zhao, J. Electrochem. Soc. 156 (2009) A917.
[6] L. Wu, X.H. Li, Z.X. Wang, J. Power Sources 189 (2009) 681.
[7] W.B. Luo, F. Zhou, X.M. Zhao, Chem. Mater. 22 (2010) 1164.
[8] W.B. Luo, J.R. Dahn, Electrochim. Acta 54 (2009) 4655.
[9] H. Yang, H. Bang, K. Amine, J. Prakash, J. Electrochem. Soc. 152 (2005) A73.
[10] H. Yang, S. Amiruddin, H. Bang, J. Ind. Eng. Chem. 12 (2006) 12.
[11] H. Yang, X.D. Shen, J. Power Sources 167 (2007) 515.
[12] M. Lu, H. Cheng, Y. Yang, Electrochim. Acta 53 (2008) 3539.
[13] R. Fong, U. von Sacken, J. Electrochem. Soc. 137 (1990) 2009.
[14] T. Ohzuku, A. Ueda, N. Yamamoto, J. Electrochem. Soc. 142 (1995) 1431.
[15] S. Pyunll, S.W. Kin, H.C. Shin, J. Power Sources 81 (1999) 248.
[16] A.D. Pasquier, A. Laforgue, J. Power Sources 125 (2004) 95.
[17] K. Zaghib, M. Simoneau, M. Armand, J. Power Sources 81 (1999) 300.
[18] S. Ma, H. Noguchi, J. Electrochem. Soc. 148 (2001) 589.
[19] D. Permunage, K.M. Abraham, J. Electrochem. Soc. 145 (1998) 2609.
[20] H.G. Jung, S.T. Myung, C.S. Yoon, Energy Environ. Sci. 4 (2011) 1345.
[21] H.Y. Yu, X.F. Zhang, A.F. Jalbout, Electrochim. Acta 53 (2008) 4200.
[22] Z.J. Lin, X.B. Hu, Y.J. Huai, Solid State Ionics 181 (2010) 412.
[23] J. Wolfenstine, J.L. Allen, J. Power Sources 180 (2008) 582.
[24] X. Li, M.Z. Qu, Y.J. Huai, Electrochim. Acta 55 (2010) 2978.
[25] H. Ge, N. Li, D.Y. Li, Electrochem. Commun. 10 (2008) 719.
[26] A. Sivashanmugam, S. Sivashanmugam, Mater. Res. Bull. 46 (2011) 492.
[27] M.W. Raja, S. Mahanty, M. Kundu, J. Alloys Compd. 468 (2009) 258.
[28] C.M. Shen, X.G. Zhang, Y.K. Zhou, Mater. Chem. Phys. 78 (2002) 437.
[29] G.F. Yan, H.S. Fang, H.J. Zhao, J. Alloys Compd. 470 (2009) 544.
[30] C.H. Jiang, M. Ichihara, I. Honma, Electrochim. Acta 52 (2007) 6470.
[31] K. Nakhara, Nakajima S R., T. Matsushima, H. Majima, Power Sources J. 117 (2003) 131.
[32] K.C. Hsiao, S.C. Liao, J.M. Chen, Electrochim. Acta 53 (2008) 7242.
[33] S.H. Ju, Y.C. Kang, J. Phys. Chem. Solids 70 (2009) 40.
[34] D. Yoshikawa, Y. Kadoma, J.M. Kim, Electrochim. Acta 55 (2010) 1872.
[35] T. Ogihara, M. Yamada, A. Fujita, Mater. Res. Bull. 46 (2011) 796.
[36] J.Z. Chen, L. Yang, S.H. Fang, Electrochim. Acta 55 (2010) 6596.
[37] Y.F. Tang, L. Yang, Z. Qiu, Electrochem. Commun. 10 (2008) 1513.
[38] M.V. Shankar, T. Kako, D.F. Wang, J.H. Ye, J. Colloid Interface Sci. 31 (2009) 132.
[39] N. Sasirekha, B. Rajesh, Y.W. Chen, Thin Solid Films 518 (2009) 43.
[40] L. Ge, M.X. Xu, H.B. Fang, M. Sun, Appl. Surf. Sci. 253 (2006) 720.
[41] F.X. Wu, X.H. Li, Z.X. Wang, Int. J. Miner. Process. 98 (2011) 106.
[42] F.X. Wu, X.H. Li, Z.X. Wang, J. Alloys Compd. 509 (2011) 3711.
[43] H. Ichinose, M. Terasaki, H. Katsuki, J. Ceram. Soc. Jpn. 104 (1996) 715.
[44] C. Lai, Y.Y. Dou, J. Power Sources 195 (2010) 3676.
[45] Y.M. Lin, P.R. Abel, J. Phys. Chem. C 115 (2011) 2585.
[46] X. Li, C. Lai, Electrochim. Acta 56 (2011) 9152.
[47] A.J. Bard, L.R. Faulkner, Electrochemical Methods, 2nd ed., Wiley, 2001, p. 231.
[48] Y.H. Rho, K. Kanamura, J. Solid State Chem. 177 (2004) 2094.
[49] T. Yuan, R. Cai, Ceram. Int. 35 (2009) 1757.